

ENGINEERING TRIPOS PART IIB

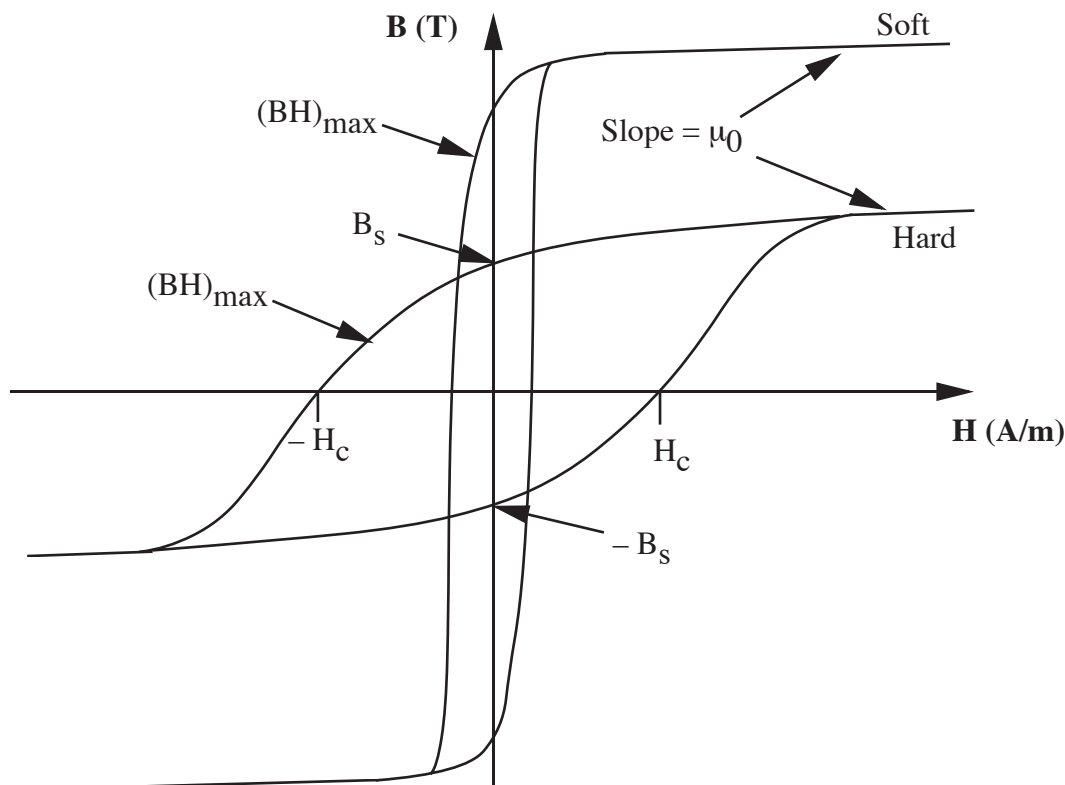
Monday 6th May 2013

9 to 10.30

Module 4C3: ELECTRICAL AND NANO MATERIALS

SOLUTIONS

1(a)(i) Pinning centres in permanent magnet materials restrict the movement of magnetic domains, which, in turn, increases the coercive force, H_c , of the material. This increases the resistance of the permanent magnet to demagnetizing effects. Pinning centres in permanent magnets take the form primarily of precipitates, such as those that resist the motion of dislocations in metals. Exactly the same effect impeded the movement of domain walls in permanent magnets. As a result, magnetic materials that contain a high density of pinning centres, such as Sm-Co and Nd-B-Fe, retain their magnetization and are mechanically hard. Permanent magnets with relatively few pinning centres, on the other hand, demagnetize easily and are mechanically soft. Hard permanent magnets are used for thin flat magnets (i.e. with a high demag. factor), such as fridge magnets. Soft magnetic materials, such as Fe, therefore, are suitable for applications in the form of long, thin cylinders, magnetised axially.

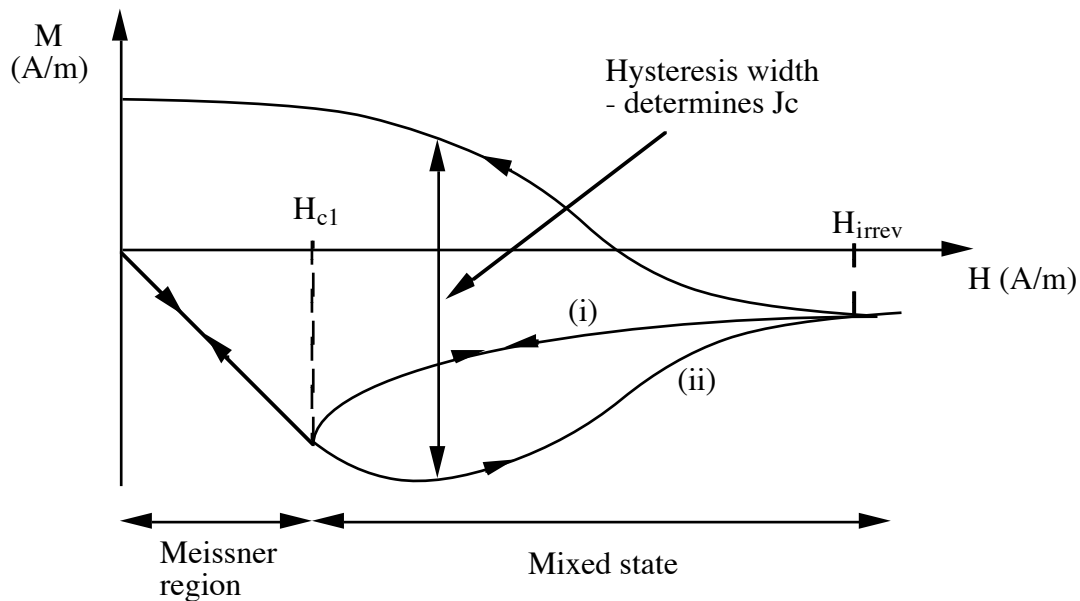


[20%]

(ii) Pinning centres in bulk YBCO superconductors take the form primarily of oxygen vacancies and/or second phase inclusions, of which the Y_2BaCuO_5 (Y-211) phase is the most common. These pinning centres pin individual flux quanta (fluxons, or quantised lines of magnetic flux that exist in type II superconductors). Flux lines move (and hence

generate loss) when the Lorentz force ($=\mathbf{B} \wedge \mathbf{J}$) overcomes the pinning force, which determines the critical current density, J_c , of the superconductor. Hence, J_c is directly proportional to the number and strength of flux pinning centres in the bulk microstructure. The optimum pinning centre geometry is approximately that of the diameter of a fluxon, which is around 10 nm in YBCO at 77 K. Pinning centres impede the motion of flux lines, which leads to the formation of a gradient, dB/dz , in flux density through the thickness of slab geometry. According to the Bean model, J_c flows where field penetrates the bulk material, and is proportional to the magnitude of the local field gradient.

The variation of magnetisation with applied field at a given temperature for (i) an 'ideal' type II superconductor (no flux pinning) and (ii) a type II superconductor which contains magnetic flux pinning centres is as follows:



[20%]

(b) The relationship between demagnetising field, H_m , of a magnetic material, applied field, H_0 , and sample magnetisation, M , is given by;

$$H_m = H_0 - NM$$

$$B_m = \mu_0 (H_m + M) \quad (i)$$

$$H_m = H_0 - NM$$

For no applied field, $H_0 = 0$, therefore;

$$H_m = - NM \quad \Rightarrow \quad M = - H_m/N \quad (ii)$$

Need $B_m (H_m)$ to plot on B-H curve.

Substitute (ii) into (i);
$$B_m = \mu_0 \left(H_m - \frac{H_m}{N} \right)$$

i.e.
$$B_m = \mu_0 H_m \left(\frac{N-1}{N} \right) \quad [15\%]$$

A sphere has a demagnetising factor of 1/3. Hence $(N-1)/N = -2$ and $B_m = -2 \mu_0 H_m$. The intersection of a straight line, gradient $-2 \mu_0$ with the B-H curve for Alcomax III (Electrical Data Book) gives the following approximate values;

$$B_m = 0.15 \text{ T} \quad H_m = -5.25 \times 10^4 \text{ A m}^{-1}$$

Also, $M = -H_m/N \quad M = -\frac{-5.25 \times 10^4}{1/3} = 1.6 \times 10^5 \text{ A m}^{-1} \quad [15\%]$

(c) Magnetic flux density at the centre of a long superconducting cylinder of YBCO of diameter 2 cm, carrying a uniform circumferential current density of $3 \times 10^4 \text{ Acm}^{-2}$ at 77 K is given by;

$$B = \frac{\mu_0 J_c d}{2} = \frac{4\pi \times 10^{-7} \times 10 \times 10^7 \times 0.02}{2} = 1.24 \text{ T}$$

(From the notes, $d =$ the cylinder diameter/2). This is significantly larger than that generated by the Alcomax III sphere in part (b).

The main practical difficulty in using the field generated by a hollow cylindrical superconductor is the inaccessibility of the field at its centre. The field at the end of the cylinder is much more accessible, although this falls to half the value at the centre. The second practical difficulty is associated with the need to cool the superconductor below its transition temperature. The need for a cryostat limits proximity to the superconductor. [30%]

2(a) Pyroelectric and piezoelectric materials are sub-classes of dielectrics, and are characterised by an asymmetry in their crystallographic structure, which leads to polar properties. The crystal structure of piezoelectric materials is characterised by a lack of centre of symmetry (i.e. they exhibit point or axial asymmetry). As a result, 20 of the known 21 dielectric structures that exhibit such a lack of centre of symmetry are piezoelectric. Pyroelectricity, on the other hand, occurs in polar dielectric materials whose structure contains at least one *axis* along which an electric dipole moment exists. Only 10 of the 21 dielectric structures, therefore, exhibit pyroelectric properties (orthorhombic, tetragonal and triclinic, for example). As a result, a pyroelectric material is necessarily piezoelectric, although the converse is not true. [20%]

(b)(i) Passive applications ($E = 0$) $P_i = d_{ijk} \sigma_{jk}$

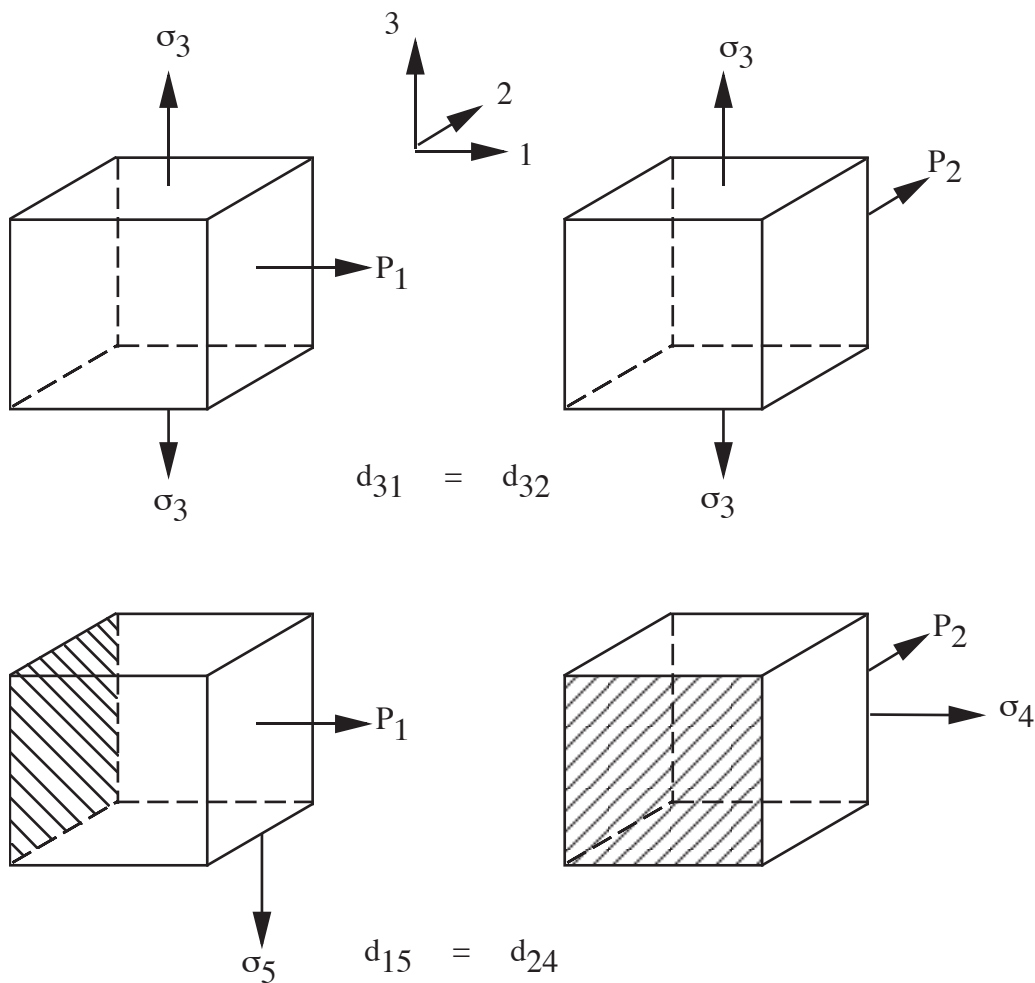
(ii) Active applications ($\sigma = 0$) $S_i = d_{ijk} E_{jk}$

where S (strain), P (change in polarisation) E (electric field) and σ (applied stress) are all variable. d is the piezoelectric coefficient, which are both constant. i, j and k take the values of 1 to 3.

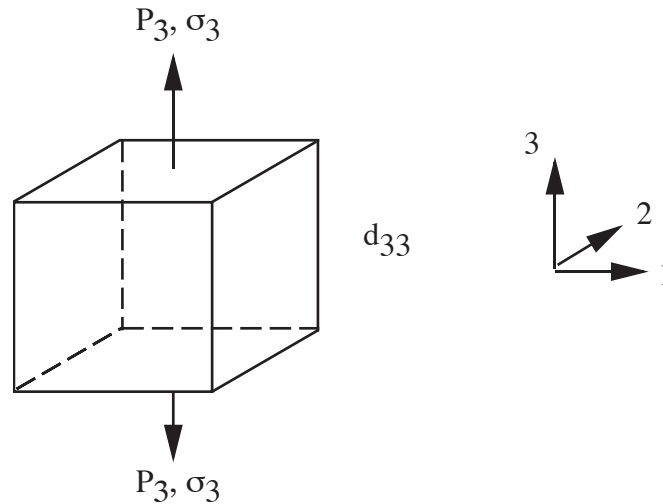
Therefore there are $3 \times 3 \times 3 = 27$ independent piezoelectric coefficients. These may be reduced to three as follows;

1. Indices i and j are interchangeable, so reduced suffix notation may be used (i.e. $d_{ijk} = d_{jik}$). As a result d_{ijk} reduces to d_{ij} with $i = 1$ to 3 and $j = 1$ to 6. This reduces the number of independent stresses (fields) to 6, and the number of piezoelectric coefficients to $3 \times 6 = 18$. Hence, for passive operation, $P_i = d_{ij} \sigma_j$

The number of modes is limited further by crystal structure and geometry for piezoelectric elements manufactured in the form of thin plates. As a result there are only 5 piezoelectric coefficients that are non-zero. These are $d_{13}, d_{23}, d_{33}, d_{15}$ and d_{24} . Finally, by symmetry, $d_{13} = d_{23}$ and $d_{15} = d_{24}$, leaving three coefficients. d_{31} and d_{15} ;



d_{33} ;



[35%]

(c) Modes of operation of piezoelectric device for the given applications;

(i) Longitudinal mode operation for a microphone (couples via d_{31}). This amplifies the signal by the aspect ratio of the piezoelectric element.

(ii) Thickness mode operation for a spark igniter (couples via d_{33}). This give the biggest change in polarisation for an applied stress.

(iii) Shear mode operation for an accelerometer (couples via d_{15}). This is insensitive to pyroelectric effects which is necessary for low noise applications.

[15%]

(d) $P = \chi E + d \sigma$ hence $\left(\frac{\partial P}{\partial \sigma}\right)_E = d$, $\Delta P = d \Delta \sigma$

$$\Delta P = \Delta Q/A, \quad \Delta \sigma = \Delta F/A, \quad \Delta Q = C \Delta V, \quad C = \frac{\epsilon_0 \epsilon A}{t}$$

i.e. $\Delta P = \frac{\Delta Q}{A} = d \frac{\Delta F}{A}$ $\Delta Q = d \Delta F = C \Delta V$

$$\Delta V = \frac{d t \Delta F}{\epsilon_0 \epsilon A} = \frac{t \Delta F}{\epsilon_0 A} \times \frac{d}{\epsilon}$$

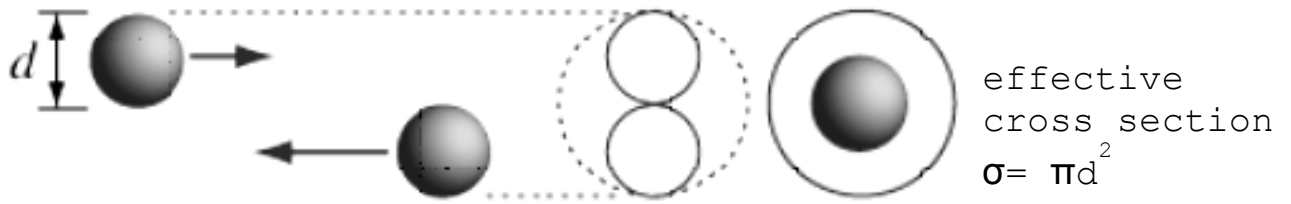
d/ϵ is the material figure of merit. In rank order for thickness mode operation;

Material	Density kg cm ⁻³	ϵ	d_{33} pC N ⁻¹	d_{33}/ϵ pC N ⁻¹
PT	7830	170	51	0.300
PZT-4	7750	1300	289	0.222
PZT-8	7600	1000	215	0.215
PZT-5	7500	3400	593	0.174
BT1	5700	1000	120	0.120

Note that the density is not required.

[30%]

3 (a) Derivation of mean free path λ (see lecture notes)

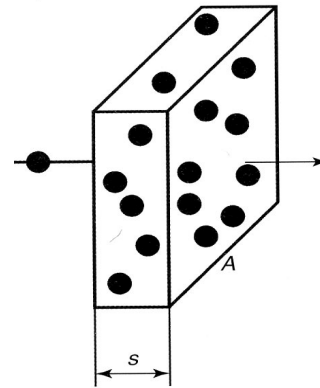


total collision area = $N \times \sigma = n \times A \times s \times \sigma$,

where n is number density of gas, σ is effective cross section and $V = A \times s$ is volume.

If total collision area equals A , then $s = \lambda$, hence

$$\lambda = \frac{1}{n\sigma} = \frac{1}{\pi d^2 n}$$



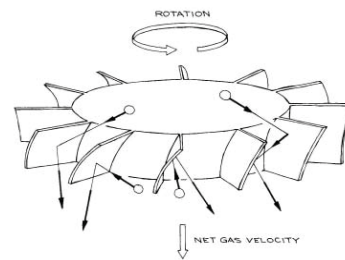
Taking relative velocities for a homogeneous maxwellian gas into account, this value for λ reduces by a factor of $\sqrt{2}$

λ for atmospheric pressure at RT: $d = 0.5 \text{ nm}$, use ideal gas approximation: $n = p/kT$

$$\lambda_{atm} = \frac{kT}{\pi d^2 p} \approx 50 \text{ nm}$$

[25%]

(b) The pumping effect of a turbomolecular pump is based upon the transfer of momentum from the rapidly rotating blades to the gas molecules being pumped. The rotor has angled blades (see Fig.), which drive gas molecules into stator, and repeated rotor/stator stages towards the outlet. Turbomolecular pumps are kinetic vacuum pumps and as their name implies require a molecular flow pressure regime, i.e. λ must be larger than the spacing between the rotating and stationary surfaces. As seen in (a):



$$\lambda \propto \frac{1}{p}$$

hence pump design has decreasing blade spacing towards outlet. At atmospheric pressure $\lambda \approx 50 \text{ nm}$, which is difficult to implement as blade clearance, so turbomolecular pump typically requires a backing pump attached to its outlet.

[20%]

(c) Al is typically deposited by PVD. Evaporation is "line-of-sight", i.e. typically shows poor step coverage, unless sample is heated and/or rotated. Hence preferred method is sputtering, for which at typical pressures of 10-100 mTorr λ is shorter than for evaporation into high vacuum, ie step coverage is improved (and can be further improved by eg sample heating). For description of sputtering, see lecture notes. [15%]

(d) (i) impingement flux J , ie number of water molecules that hit chip surface per unit area per unit time is (see lecture notes):

$$J = \frac{1}{4} n \bar{v} = \frac{p}{\sqrt{2\pi mkT}}$$

The number of atoms in a monolayer N_{mono} is approx. $1/d^2$, and it will take time $t_{\text{mono}} = N_{\text{mono}}/J$ for monolayer coverage of chip.

$d=0.5$ nm, hence $N_{\text{mono}} \approx 1/d^2 = 4 \times 10^{18} \text{ m}^{-2}$; $t_{\text{mono}} = 600\text{s}$,

$$J = \frac{N_{\text{mono}}}{t_{\text{mono}}} = \frac{p}{\sqrt{2\pi mkT}}$$

which at RT and for $m=18u$, gives background pressure $p=2 \times 10^{-7}$ Pa [25%]

(ii) X-ray photoemission spectroscopy (XPS) would be suitable to detect adsorbed water and surface oxidation (see lecture notes). X-ray absorption results thereby in the emission of photoelectrons (see photoelectric effect), the energy of which is characteristic of element and its chemical state. A typical XPS spectrum plots electron yield vs binding energy and XPS line-widths are narrow enough to resolve chemical shifts. Due to the limited escape depth of photo electrons, XPS is a highly surface sensitive technique. [15%]

4(a) Si

Advantages: cheap, SiO_2 as oxide, versatility, moderate speed, bipolar.

Disadvantages: slow, indirect gap, not opto-electronic.

GaAs

Advantages: faster than GaAs, lower effective mass.

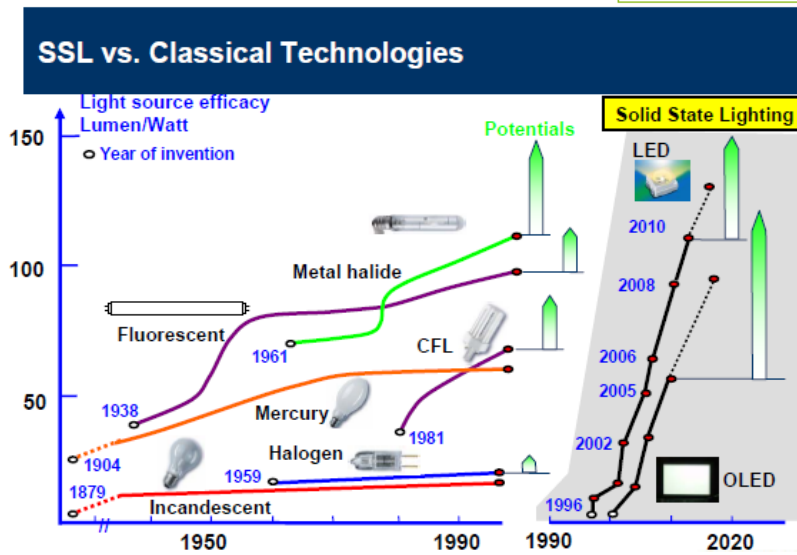
Disadvantages: cost, small wafer sizes, bad oxide, not passivated, complicated defects.

GaN

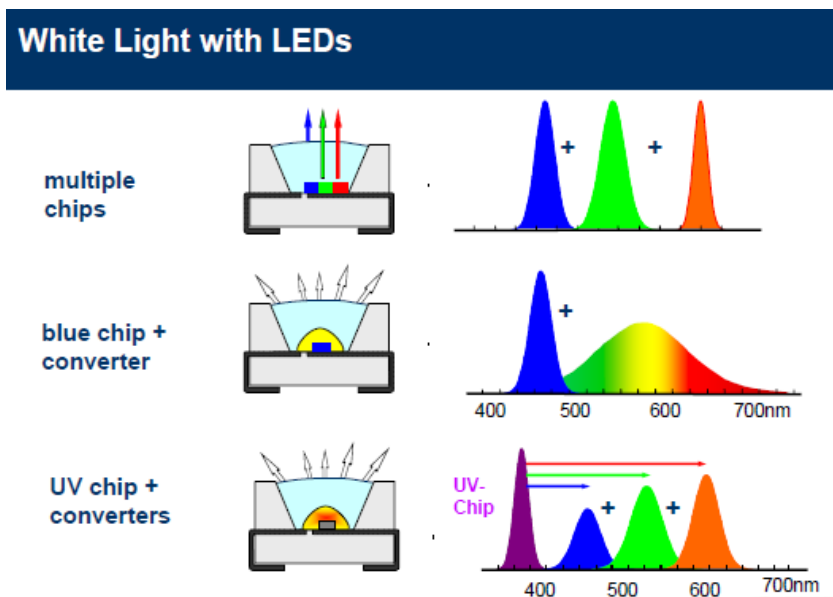
Advantages: faster than Si, high thermal conductivity, high breakdown field, bipolar, high figure of merit for power devices, wide band gap, direct gap, opto-electronic, LEDs.

Disadvantages: poor oxide, deep acceptors, processing, cost, small wafer sizes. [25%]

(b) Because of environmental reasons, there is search for more efficient light technologies, leading to GaN based LEDS and eventually OLEDs. Some of technologies are given in the following diagram;

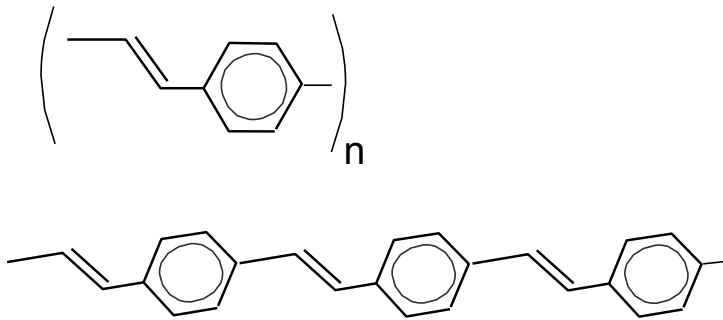
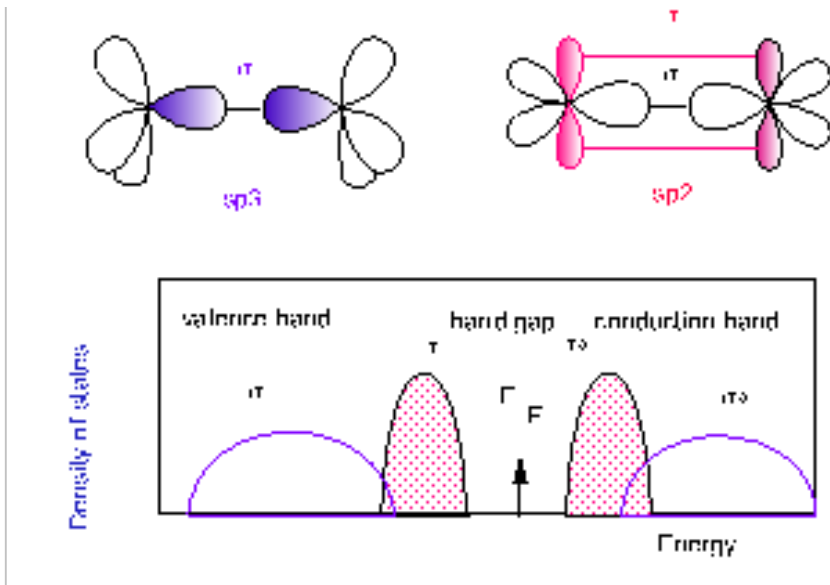


Three ways to obtain white light from LEDs are summarised in the following diagram. GaN LED is an inorganic LED.



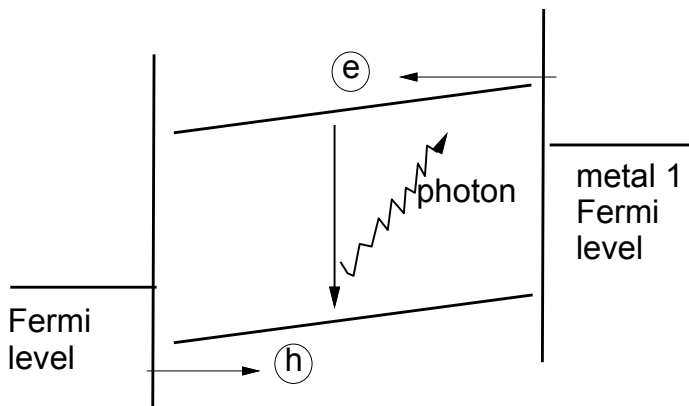
[25%]

(c) Bond and band diagrams to describe conduction occurs in organic semiconductors are as follows;



Conduction occurs at the top of the valence band (VB) or bottom of the conduction band (CB), that is the pi states of double bonds. Hence the conjugate carbon bonds in the band diagram. [25%]

(d) Organic semiconductors act in organic light emitting diodes as follows;

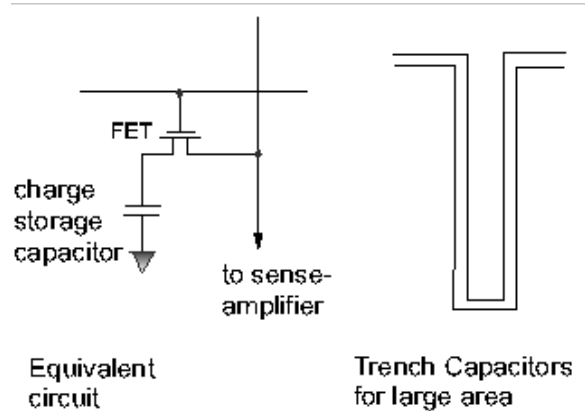


Light emission occurs by recombination of electrons and holes in the bulk of the OLED semiconductor. But, unlike in GaAs, the carriers are not provided by doping, but are injected into each electrode, by the design of the band edge energies of the 2 contact metals, high work function for anode, low work function for cathode.

[25%]

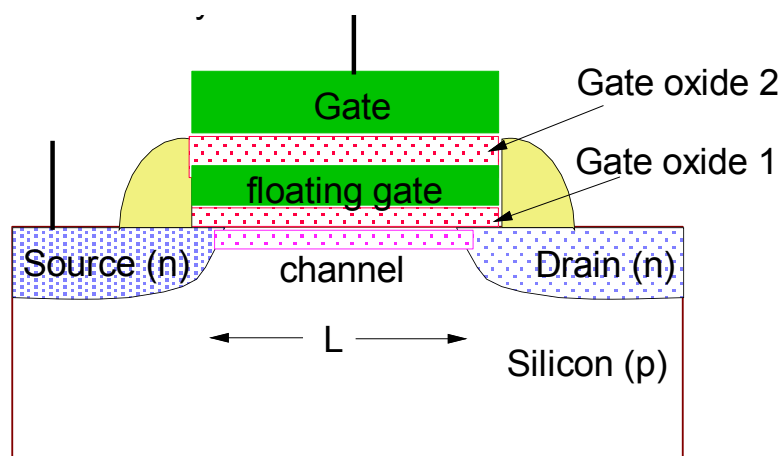
5 (a) Volatile is temporary memory, whereas non-volatile is permanent memory.

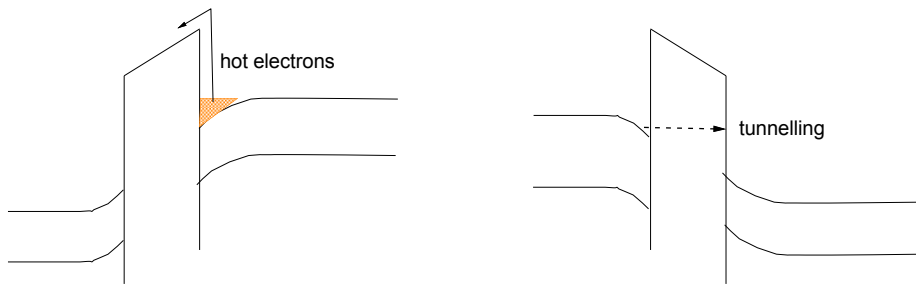
Volatile = DRAM:



The storage mechanism is refreshing/charging of the capacitor.

Non-volatile = Flash:

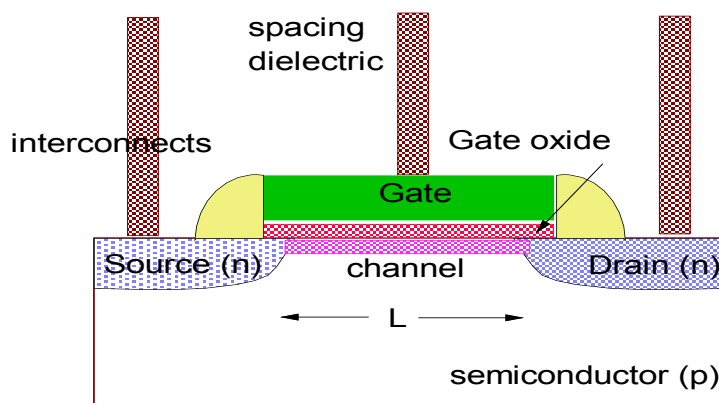




The storage mechanism is writing/erasing charge in the floating gate. Reading is via the (main) gate voltage.

[35%]

(b)



channel = Si

gate electrode = doped poly Si

interconnects = Cu

drain, source regions = doped Si

gate oxide = SiO_2

[15%]

(c) In a planar MOSFET SiO_2 is used for three main purposes;

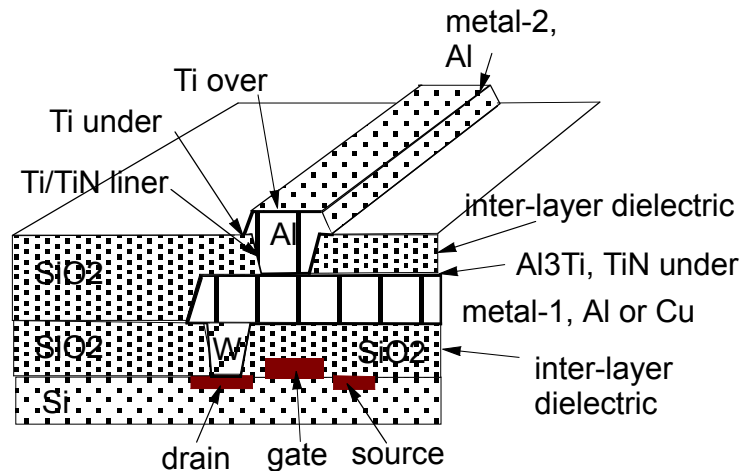
1. The gate oxide dielectric;
2. The spacing /inter-interconnect oxide dielectric;
3. The passivant.

The gate oxide needs higher capacitance, so higher K. This increases the gate-channel capacitance. So for given gate voltage, a larger charge density is induced in the channel, and so this increases the drain current in proportion. Hence, HfO_2 is used.

The spacing dielectric needs lower capacitance, so lower K. This reduces the capacitance between the wires in the IC, so for a fixed R in the wires, the RC time constant is reduced, and this reduces the delays in signals. Hence, SiO_2/F and SiOCH_x are used.

[15%]

(d) The components of a MOSFET are as follows;



The following changes would result in improved performance;

1. Semiconductor. Initially Si, now strained Si/Ge for high mobility, next InGaAs for higher mobility.
2. Channel -> high mobility channel – GaAs or Ge (mobility)
This would increase the mobility of the carriers and therefore increase the transconductance of the MOSFET.
3. Gate oxide -> high K oxide (raise C)
This would increase the gate-channel capacitance. So, for a given voltage, a larger charge density is induced in the channel, which would increase the drain current in proportion.
4. Intermetal dielectric -> low K oxide (lower C)
This would reduce the capacitance between the wires in the IC, so for a fixed R in the wires, the RC time constant is reduced, which reduces delays in signal transmission.
5. Interconnects, Al -> Cu -> carbon nanotubes (raise current density)
Cu takes a higher max current density, so this allows a large current density to flow between different FETs. Needs diffusion barriers. CNTs takes even higher J.
6. Contact metals -> silicides (compatibility)
The use of silicon would reduce the resistance of the source and drain contacts and their Schottky barrier heights, so lowering the overall resistance of the circuit. This would reduce power loss and RC delays.

Gate electrode. Until 1970 Al, then highly doped (metallic) poly-Si, now metal (eg TiN, silicides). Use of silicides reduces the resistance of source and drain contacts and their Schottky barrier heights, so lowering the overall resistance round the circuit.

[35%]